APSB
Acta Pharmaceutica Sinica B
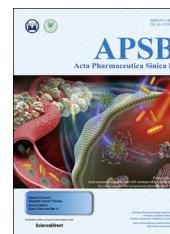
ORIGINAL ARTICLE

Development of polyvinylpyrrolidone/paclitaxel self-assemblies for breast cancer

CrossMark

Pallabita Chowdhury, Prashanth K.B. Nagesh, Sheema Khan, Bilal B. Hafeez, Subhash C. Chauhan, Meena Jaggi, Murali M. Yallapu*

Department of Pharmaceutical Sciences and Center for Cancer Research, University of Tennessee Health Science Center, Memphis, TN 38163, USA

Abstract The goal of this investigation was to develop and demonstrate a polymer/paclitaxel self-assembly (PTX-SA) formulation. Polymer/PTX-SAs were screened based on smaller size of formulation using dynamic light scattering analysis. Additionally, fluorescence microscopy and flow cytometry studies exhibited that polyvinylpyrrolidone (PVP)-based PTX-SAs (PVP/PTX-SAs) had superior cellular internalization capability in MCF7 and MDA-MB-231 breast cancer cells. The optimized PVP/PTX-SAs exhibited less toxicity to human red blood cells indicating a suitable formulation for reducing systemic toxicity. The formation of PVP and PTX self-assemblies was confirmed using fluorescence quenching and transmission electron microscopy which indicated that the PVP/PTX-SAs were spherical in shape with an average size range of 53.81 nm as detected by transmission electron microscopy (TEM). FTIR spectral analysis demonstrates incorporation of polymer and paclitaxel functional groups in PVP/PTX-SAs. Both proliferation (MTS) and clonogenic (colony formation) assays were used to validate superior anticancer activity of PVP/PTX-SAs in breast cancer cells over paclitaxel. Such superior anticancer activity was also demonstrated by downregulation of the expression of pro-survival protein (Bcl-xL), upregulation of apoptosis-associated proteins (Bid, Bax, cleaved caspase 7, and cleaved PARP) and β-tubulin stabilization. These results support the hypothesis that PVP/PTX-SAs improved paclitaxel delivery to cancer cells.

*Corresponding author. Tel.: +901 448 1536; fax: +1 901 448 4731.
  E-mail address: myallapu@uthsc.edu (Murali M. Yallapu).

1. Introduction

Breast cancer (BC) remains the most commonly diagnosed cancer among women in the United States[1]. The most recent data on cancer incidence, mortality, and survival by the American Cancer Society estimated that there will be 63,410 *in situ* cases and 252,710 invasive cases with 40,610 deaths occurring in the US in 2017[1]. Paclitaxel (PTX), is a natural compound derived from the bark of *Taxus Brevifolia*, antimicrotubule and well-established chemotherapeutic agent, which exhibits a broad spectrum of anticancer activity against breast cancer, prostate cancer, leukemia, non-small cell lung cancer, and ovarian cancer[2,3]. Due to its hydrophobicity, it is often formulated with Cremophor EL in ethanol solution, *i.e.*, Taxol®, which limits clinical use due to its adverse side effects, such as increased risk for fatal hypersensitivity reactions[4], non-linear pharmacokinetics[5], prolonged peripheral neuropathy[6], and myelosuppression[7], leading to less bioavailability at the tumor site and therefore reduced efficacy for its action against tumor cells[6,8,9]. Other common side effects of PTX treatment include vomiting, nausea, loss of appetite, and joint pain.

In order to circumvent these side effects, various alternative nanoparticle-based PTX formulations were developed. One of the most widely used formulations is Abraxane®, which is a Cremophor-free and albumin-bound paclitaxel nanoparticle formulation (diameter ~120 nm), developed as an alternative formulation to PTX (Taxol®)[2]. This serum albumin bound PTX nanoformulation is approved by the US Food and Drug Administration for the treatment of breast, lung and pancreatic cancer. This formulation facilitates crossing across endothelial layers of cells and achieves 33% higher PTX concentration at the tumor site[10]. Additionally, Abraxane® was able to increase the maximum tolerated dose (MTD) by 70–80% compared to PTX. Another PTX nanoformulation, Genexol PM® was approved in South Korea for first line treatment for metastatic or recurrent breast cancer, non-small cell lung cancer, and also used in combination with carboplatin for ovarian cancer. It is a polymeric micellar formulation of polyethylene glycol (PEG), poly(D,L-lactide), and PTX. NK-105 (block copolymer of PEG and polyaspartate modified with 4-phenyl-1-butanol with PTX) is another nanoparticular micellar formulation that has entered phase III clinical trial for metastatic and recurrent breast cancer. NK-105 exhibits prolonged circulation, enhanced area under the curve (AUC) by 20 times in contrast to PTX and also had higher antitumor activity[11]. Other clinically used (or under clinical development) PTX formulations/nanoformulations include Paclical® (paclitaxel combined with Oasmia's excipient technology XR17)[12], Lipusu® (paclitaxel liposome)[13], paclitaxel injection concentrate for nanodispersion (PICN)[14], SB05 (positively charged liposome embedded with paclitaxel)[15], LEP-ETU (liposome-entrapped paclitaxel)[16], and Triolimus (micelle containing paclitaxel, rapamycin and 17-AAG)[17]. Self-assembly and solid dispersion techniques were a common approach to generate these clinically relevant PTX nanoformulations.

The goal of this study was to develop a PTX nanoformulation using a polymer-based self-assembly technique, using a polymer excipient already in use in the pharmaceutical industry. The self-assembly process is a well-established, simple, and rapid fabrication method to generate nanosized architecture materials for drug delivery applications[18–20]. We selected 8 biocompatible polymers for generating self-assembled polymer/PTX nanoformulations. Table 1 provides structures of polymers used in this study. Among those, Poloxamer 188 [a nonionic copolymer containing hydrophobic poly

(propylene oxide) (PPO) and two hydrophilic poly(ethylene oxide) (PEO) units] is widely used for generating micelles by the self-assembling technique where the PEO units align at the outer lining and PPO falls in the inner core leading to the formation of micelle above the critical micellar concentration. We expect polymeric micelles will be formed using Poloxamer 188[21]. Whereas, the other seven polymers were commonly used as drug delivery carriers for generating solid dispersions or polymeric nanoparticles[22–24]. The motive of this study is to minimize any other external agents being added for the formulation development. Self-assembly is a process where the various components are held together by inter-particulate assembly[25]. There are reports stating that synergistic interactions between self-organizing particles and a self-assembling matrix material can lead to hierarchically ordered structures[26]. Accordingly, we developed nanostructured formulations of hierarchical order using PTX and various polymers without any external reagents or binders. Such self-assembly formulations may have the potential to circumvent the shortcomings of PTX and provide advantages such as: ease of preparation; smaller particle size; an efficient binding ability to PTX; and enhanced particle uptake in cancer cells. In this investigation, we report an optimized PVP/PTX-SA formulation with enhanced cellular uptake and superior *in vitro* cytotoxicity in breast cancer cells, compared to PTX.

2. Materials and methods

2.1. Materials

All laboratory reagents, solvents, and chemicals were purchased from Sigma–Aldrich Co. (St. Louis, MO, USA) or Fisher Scientific (Pittsburgh, PA, USA) unless otherwise mentioned. Cell culture plastics were purchased from Sarstedt, Inc. (Newton, NC, USA). All chemicals were used as received without any further purification.
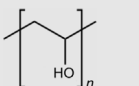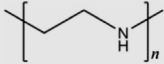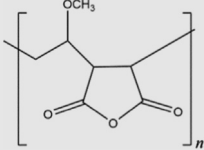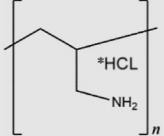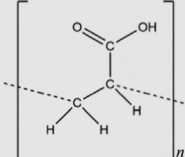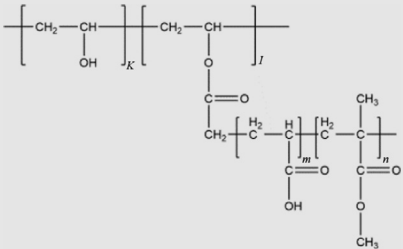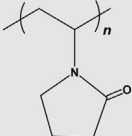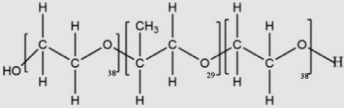
2.2. Cell culture, growth conditions and treatment

Breast cancer cell lines (MCF7 and MDA-MB-231) were obtained through American Type Culture Collection (Manassas, VA, USA) and stored as low passage frozen aliquots upon cell culture expansion. These cell lines were thawed and cultured under sterile conditions for all experiments (<3–4 months after thawing). Both cell lines were cultured in Dulbecco's modified Eagle's medium-high glucose (DMEM-Hi) medium containing 4.5 g/L of glucose, 10 nmol/L of nonessential amino acids, 100 nmol/L of sodium pyruvate, 1× antibiotic/antimycotic (Gibco, Thermo Fisher Scientific, Grand Island, NY, USA) and 10% heat-inactivated fetal bovine serum (FBS, Atlanta Biologicals, Lawrenceville, GA, USA) at 37 °C in a humidified atmosphere (5% CO_2 and 95% air condition, ThermoScientific, Waltham, USA). In all cell culture experiments, monodispersed cell lines after trypsinization were plated on either 6-, 12-, or 96-well plates, and were allowed to adhere overnight to the plate before implementing treatments.

2.3. Preparation of polymer-PTX-SAs (Poly/PTX-SAs)

Eight polymer-based drug delivery vehicles, such as polyvinyl alcohol (PVA, MW 31,000–50,000), polyvinylpyrrolidone (PVP, MW 40,000), polyethyleneimine (PEI, MW 25,000), poly(methyl vinyl ether-alt-maleic hydrochloride) (PMEAVH, MW 216,000),

Table 1   Polymers employed for self-assembling PTX to produce polymer/PTX self-assembly nanoparticles.

No.	Name of polymer	Structure of Polymer
1	Polyvinyl alcohol (PVA)	
2	Polyethyleneimine (PEI)	
3	Poly(methyl vinyl ether-alt-maleic hydrochloride) (PMEAVH)	
4	Poly(allylamine hydrochloride) (PA-HCl)	
5	Polyacrylic acid (PAA)	
6	Povacoat F (polyvinyl alcohol-acrylic acid-methyl methacrylate) copolymer	
7	Polyvinylpyrrolidone (PVP)	
8	Poloxamer 188 (P188)	

poly(allylamine hydrochloride) (PA-HCl, MW 17,500), Poloxamer 188 (Kolliphor® P 188, P188), polyacrylic acid (PAA, MW 100,000), and Povacoat F (polyvinyl alcohol-acrylic acid-methyl methacrylate copolymer: Type F, MW 40,000, a gift sample received from Daido Chemical Co., Osaka, Japan), were used in the PTX self-assembly formation. The self-assembly formation technique is followed by solvent evaporation. Briefly, 5 mg of polymer was dissolved in 1 mL aqueous medium in 8 mL glass vial under continuous stirring at 400 rpm on a stir plate (Benchmark digital magnetic hotplate stirrer, ABC Scientific, Glendale, CA, USA). To this solution, 100 μL of PTX dissolved in acetone (1 mg/mL) was added slowly (dropwise) and the speed increased to 900 rpm. The obtained solution was stirred overnight to evaporate the acetone resulting in formation of self-assembled nanoparticles comprised of assembled polymer chains and PTX, *i.e.*, referred to as polymer/paclitaxel self-assemblies (Poly/PTX-SAs). The resultant Poly/PTX-SAs solution was kept refrigerated

and used within a week. For all *in vitro* cell culture experiments, a fresh batch of Poly/PTX-SAs was used in order to protect PTX activity in the formulations.

2.4.   Characterization of Poly/PTX-SAs

2.4.1.   Particle size and zeta potential

The average particle size, particle distribution and zeta potential of the prepared PTX-SA formulations were measured by the dynamic light scattering (DLS) principle using Zetasizer (Nano ZS, Malvern Instruments, Malvern, UK). These measurements were done as previously reported[27], briefly 50 μL of freshly prepared Poly/PTX-SA nanoparticle suspension was dispersed in deionized water and was probe sonicated (VirSonic Ultrasonic Cell Disrupter 100, VirTis) for 30 s. Probe sonication procedure is commonly applied in formulation development for the formation of nanoparticles and

homogeneous solution which minimizes the interaction of aggregated nanoparticles and to disperse well but not to break particles into smaller particles. Additionally, a short span of sonication is subjected to ensure that particle suspension is homogeneous in nature. Particle size measurements were performed in water for 3 min at 25 °C. An average diameter and distribution of particle size was determined from triplicated runs. In a similar way, zeta potential was measured using nanoparticle suspension diluted with 1× phosphate-buffered saline (PBS). The zeta potential of nanoparticle formulations was also based on the average of 3 readings (each reading = 30 runs).

2.4.2. Transmission electron microscopy

The size and surface morphology of PVP/PTX-SAs were investigated by JEOL 200EX transmission electron microscopy (TEM, JEOL Ltd, Tokyo, Japan) operating at 80 kV. For this, 100 µL of PVP/PTX-SA suspension was dispersed in 1 mL of water, were probe sonicated for 30 s. On a 150 mesh standard TEM grid (Electron Microscopy Sciences, PA, USA), a 20 µL aliquot of the PVP/PTX-SAs was carefully placed on the shiny side of the grid. It was stained using 2% (w/v) uranyl acetate solution. The excess amount of formulation was removed using filter paper and the grid was allowed to air dry followed by imaging using an AMT camera at a direct magnification of 100,000× under the TEM system.

2.4.3. Spectral analysis

A Fourier transform infrared (FTIR) spectrum was employed to determine the formation of PVP/PTX-SAs. FTIR spectral data were acquired on the Universal ATR sampling Accessory plate using a Spectrum 100 FTIR spectrophotometer (Perkin Elmer, Waltham, MA). Samples of PVP/PTX-SAs was lyophilized to obtain dry solid particles using a Labconco Freeze Dry System (–48 °C, 133×10^{-3} m Bar; Labconco, Kansas City, MO, USA). The samples (PTX, PVP and PVP/PTX-SA) were placed on the tip of the ATR objective and spectra were obtained between 4000 and $650 \, cm^{-1}$.

2.5. Fluorescence binding

Self-assembly formation of polymer and PTX was determined on a SpectraMax Plus plate reader (Molecular Devices, Sunnyvale, CA, USA). For this study, PTX conjugated dye (PTX, Oregon Green 488 conjugate with a Flutax-2, Molecular Probes Inc., Life Technologies, OR, USA) was used, from which the fluorescence quenching of Oregon green 488 on PTX was achieved by titrating with polymeric/surfactant solutions. Intrinsic fluorescence of 5 µg/mL PTX solution in 1× PBS was titrated with 0–80 µg/mL of PVP solution. The decay in fluorescence was studied by exciting at 496 nm and emission between 450–600 nm.

2.6. Hemolysis assay

A healthy human donor blood with sodium citrate as anticoagulant was purchased from Interstate Blood Bank Inc. (Memphis, TN, USA) for the hemolysis test. The hemoglobin released from red blood cells (RBCs) upon treatment with 10 µg PTX/well or 10 µg PTX equivalent/well of Poly/PTX-SAs was quantitatively measured as described earlier[28,29]. For this assay, 200 µL of RBC suspension (8×10^5) was incubated with 10 µg/well of PTX or Poly/PTX-SAs (of similar concentration as PTX) and placed in an incubator for 60 min at 37 °C. Sodium dodecyl sulfate (SDS, 1 mg/mL) was used as a

positive control (100% lysis) while 1× PBS was used as a negative control (0%). After the incubation for 1 h, hemoglobin released into medium (supernatant, 100 µL) was collected, transferred to a 96-well plate, and absorbance was measured at 510 nm using a plate reader (Cytation 3 imaging reader, BioTeK Winooski, VT, USA). To further confirm these results qualitatively, a few drops of the treated RBC solution was smeared on a glass slide and images were captured using EVOS® FL Imaging System (AMF4300, Life Technologies, Carlsbad, CA, USA). The percentage of hemolysis was calculated using the Eq. (1):

$$Hemolysis \, (\%) = \left[\frac{Absorbance \, of \, samples - Absorbance \, of \, negative \, control}{Absorbance \, of \, positive \, control} \right] \times 100 \quad (1)$$

2.7. Cellular uptake

For this study, previously reported methods were employed for qualitative and quantitative uptake of coumarin 6 loaded in Poly-SAs in cancer cells[30,31]. In this experiment, freshly prepared coumarin 6-loaded Poly-SAs were generated by procedures described in Section 2.3. The polymer to dye ratio was kept 50:1 (5 mg of polymer and 100 µg of dye). Breast cancer cell lines, MCF7 and MDA-MB-231 (5000 cells/well with 100 µL media/well in 96-well culture plates) were seeded at 500,000 cells/well with 2 mL medium in a 6-well plate. Cells were allowed to attach to the plate and media was replaced with 5 µg (dye equivalent) coumarin 6-loaded Poly-SAs. To ensure the stability of coumarin 6 dye, such that it does not leach out of the nanoassemblies, a shorter incubation time of 3 h was selected. Since it is a comparative experiment among 8 different formulations to identify
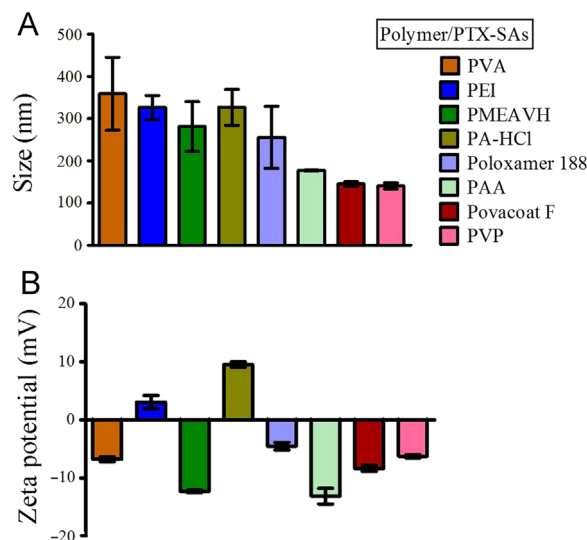
Figure 1 Particle size and zeta potential of Poly/PTX-SAs. 50 µL of Poly/PTX-SAs were dispersed in 1 mL distilled water or 1× PBS and probe sonicated for 30 s. These solutions were measured for particle size and zeta potential using dynamic light scattering at 25 °C using Zetasizer (Nano ZS, Malvern Instruments, Malvern, UK). (A) Average particle size of polymer PTX-SAs was measured for 3 min exhibiting the smallest size for PVP/PTX-SAs (140.53 nm). (B) Zeta potential of Poly/PTX-SAs was measured in 1× PBS and average of 3 readings (each reading = 30 runs) were presented. Data represented as an average of three readings that were recorded independently with error bars represented as standard error of the mean.

Figure 2 Evaluation of hemocompatibility behavior of Poly/PTX-SAs. (A) Hemocompatibility was assessed using human red blood cells by treating them for 1 h with PTX or Poly/PTX-SAs. In this experiment, sodium dodecyl sulfate (SDS, 1 mg/mL) served as a positive c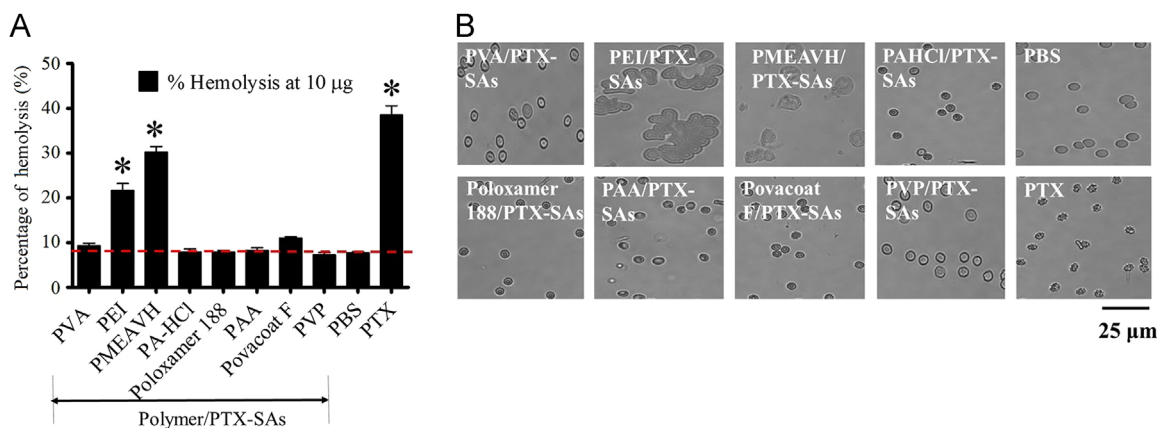ontrol (100% lysis) while 1× PBS was used as a negative control (0%). The percentage of hemolysis was calculated using our previously reported method. (B) Images of treated red blood cells on glass slide were captured using EVOS® FL Imaging System (AMF4300, Life Technologies, Carlsbad, CA, USA). PVP/PVA-PTX-SAs demonstrate intact membrane morphology in RBCs as PBS, whereas PTX and other Poly/PTX-SAs exhibited toxic behavior by disintegrating membrane structure of RBCs (Bar=25 μm). Data represented as mean ± standard error of the mean ($n = 3$), $^{*}P < 0.05$.

the best one, we have not considered coumarin 6 leaching from formulations. After a 3 h treatment, cells were washed twice with 1× PBS to remove the excess coumarin 6-loaded Poly-SAs that may be adhered to the surface of the culture plate or cells. Then, DMEM phenol red free medium was added to these treated cells and uptake of coumarin 6-loaded Poly-SAs in cells was imaged using EVOS® FL Imaging System (AMF4300, Life Technologies, Carlsbad, CA, USA). Furthermore, the quantitative uptake of coumarin 6-loaded Poly-SAs in cells was determined by trypsinizing, centrifuging and collecting the cells in 2 mL media, which were injected (50 μL cell suspension) into an Accuri C6 Flow Cytometer (Accuri Cytometer, Inc., Ann Arbor, MI, USA). Quantitative uptake of couamrin 6-SAs measurements were acquired using the fluorescence levels in FL1 channel (488 excitation, Blue laser, 530±15 nm, FITC/GFP). Standard deviations were calculated from 3 replicates.

2.8. Cell viability assay

A calorimetric CellTiter 96® aqueous one solution cell proliferation assay (MTS assay, Promega, Madison, WI) was used to examine the effect of PTX-SAs on cell proliferation of breast cancer cells. The measurement of cell viability is based on the ability of viable cells to cleave the tetrazolium compound 3-(4,5-dimethylthiazol-2-yl)-5-(3-carboxymethoxyphenyl)-2-(4-sulfophenyl)-2H-tetrazolium, salt by mitochondrial dehydrogenase. Briefly, MCF7 and MDA-MB-231 (5000 cells/well with 100 μL media/well in 96-well culture plates) were seeded in regular growth medium and allowed overnight cells to attach to the wells. These cells were treated with 1.25, 2.5, 5, 10, and 20 nmol/L PTX or PVP/PTX-SAs in order to determine the cell proliferation capability. Cell lines with no treatment served as controls, respectively. After 48 h of treatment, 20 μL of MTS reagent solution was added to the cells and incubated for 2 h at 37 °C. Absorbance reading was recorded at 490 nm using a Microplate Reader (BioTeK Cytation 3, Winooski, VT, USA). Data were plotted using cell proliferation against concentration of treatment, where the proliferation of PVP/PTX-SAs and PTX was determined by the

percentage of the absorbance of treated cells to the absorbance of control or non-treated cells. All the experiments were performed at least in triplicates.

2.9. Clonogenic assay

Clonogenic assay was performed to investigate the effect of PVP/PTX-SAs on breast cancer cells to form colonies as an *in vitro* cell survival assay based on the ability of a single cell to grow into a colony. For this study, breast cancer cells were seeded (250 cells/well) in 12-well plate and allowed 2 days to attach and start generating smaller colonies. Then, these initiated cell colonies were treated with 0.25, 0.5 and 1 nmol/L PTX and PVP/PTX-SAs for two weeks. Visible colonies were fixed, stained with hematoxylin and manually counted (~50 cells considered as a colony) as discussed earlier[27,32]. The results are presented as percentage of colonies as compared to the control (non-treated cells).

2.10. Tubulin stabilization assay

β-Tubulin stabilization assay was performed by immunofluorescence assay to examine PTX inherent tubulin binding and alteration efficacy of PVP/PTX-SAs[27]. Briefly, 25,000 cells/well were cultured in 4-well chamber slides and cultured overnight to attach to a glass slide before treatment with 5 nmol/L PTX or PVP/PTX-SAs or respective controls (DMSO or polymer) for 8 h. After treatment, cells were rinsed with 1× PBS for 3 min three times, fixed with ice-cold methanol for 20 min, blocked with 10% goat serum for 1 h. Then, cells were immunostained overnight with β-tubulin antibody (1:50 cell signaling, #CS2146) at 4 °C on a rocker with 20 oscillations/min. After incubation with primary antibody, cells were rinsed three times with 1× PBS then probed with Alexa Fluor 488 goat anti-rabbit secondary antibody (1:200, # A11008, Thermo Fisher Scientific, Waltham, USA) for 1 h. DAPI was used to counterstain nuclei of cells. Finally, the polymerization of tubulin in cells was visualized under a laser confocal microscope (Carl Zeiss LSM 710, Thornwood, NY, USA) with a 40×0.7NA oil immersion objective.

2.11. Immunoblot analysis

For immunoblot analysis, MDA-MB-231 cells (1×10^6 in 10 mL medium) were seeded in a 100 mm culture dish and treated with 10 nmol/L PTX or PVP/PTX-SAs or respective control (DMSO and PVP) for 48 h. These cells were lysed with Cell Lytic™ M reagent (Sigma–Aldrich Co., St. Louis, MO, USA), the protein concentrations were measured, and equal concentrations of total protein were separated by SDS-PAGE, and the Western blotting methods were followed as described previously[33,34]. Primary antibodies [β-actin (#4967), BAX (#2772), BID (#2003), cleaved caspase7 (#9491), BCL-XL (#2762), cleaved PARP (#9548) and MDR1/ABCB1 (#13342)] (Cell Signaling Technologies, Danvers, MA, USA) and secondary antibody (horseradish peroxidase-conjugated goat anti-mouse #7076P2 or goat anti-rabbit #7074P2 secondary antibody) (Cell Signaling) were used in this study. The specific protein bands were detected using enhanced Lumi-Light Detection Kit reagent under a Biorad ChemiDoc™ MP System (Biorad, Hercules, CA, USA).

2.12. Statistical analysis

All statistical analyses were performed with GraphPad Prism 5 Software (GraphPad Software, San Diego, CA, USA) using Student's t-test. The difference was considered to be significant for P values of <0.05. DLS (particle size and zeta potential), hemolysis, cellular uptake, and MTS assay data were expressed as mean $\pm$ standard error of the mean. All graphs were generated using GraphPad Prism 5 Software.

3. Results

3.1. Development of a suitable Poly/PTX-SA formulation for breast cancer

A successful self-assembled nanoparticle formulation may deliver therapeutic agent at the tumor site more efficiently than the parent PTX drug molecule alone. The selection of such a self-assembly carrier depends on its physico-chemical and biological characteristics. Therefore, in this investigation, we used eight commonly used pharmaceutical delivery vehicles to load PTX by the self-assembly technique which allows formation of nanoparticles. The inherent thermodynamic forces direct the nanoparticle formation without use of external agents. A similar self-assembly process was previously reported by our group for β-cyclodextrin-curcumin and poly(β-cyclodextrin)-curcumin assemblies[32,35]. These self-assembled nanoparticles are much more stabilized and thus prevent aggregation and flocculation. To further ensure that solution is homogeneous in nature we have probe sonicated the self-assembled nanoparticles[36]. The formed self-assemblies of PTX with various polymers produced particle sizes ranging from 140.53 to 358.86 nm which were measured by dynamic light scattering measurements (Fig.1A). A lower particle size self-assembly was observed with PVP/PTX-SAs (140.53 $\pm$ 7.08 nm) and Povacoat F-PTX-SAs (145.2$\pm$5.33 nm) due to strong PTX holding capacity within their polymer chain networks. High positive zeta potential formulation often induces systemic toxicity.
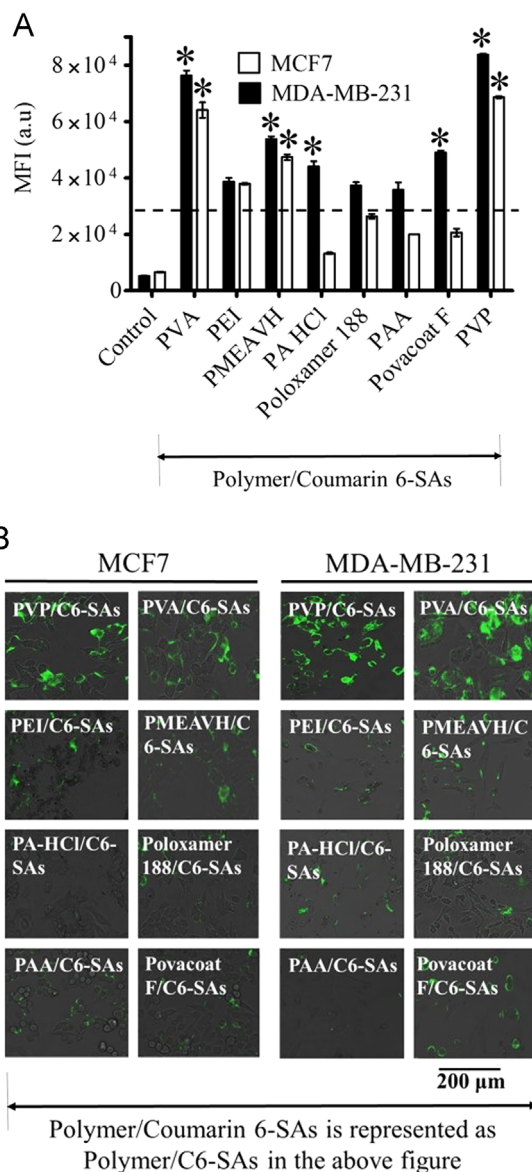

Figure 3 Cellular uptake of Poly/PTX-SAs. (A) Quantitative cellular uptake evaluation. All the cells were treated with Poly SAs loaded with coumarin 6 instead of PTX in order to evaluate fluorescent uptake in cells. BC cells (500,000) were treated with Poly/coumarin 6-SAs (5 μg dye equivalent formulations) for 3 h. These cells were trypsinized, centrifuged and collected in 2 mL media, which were injected (50 μL cell suspension) into an Accuri C6 Flow Cytometer (Accuri Cytometer, Inc., Ann Arbor, MI, USA). Mean fluorescence intensity in FL1 channel (488 excitation, Blue laser, 530 $\pm$ 15 nm, FITC/GFP) was measured. Data represented as mean $\pm$ standard error of the mean ($n = 3$), *$P < 0.05$. (B) Qualitative internalization efficiency of Poly/coumarin 6-SAs in BC cells. In above treatment condition, uptake of Poly/couamrin 6-SAs in BC cells was viewed using EVOS® FL Imaging System (AMF4300, Life Technologies, Carlsbad, CA, USA). Bar equals to 200 μm. This study suggests fluorescence intensity in the order: PVP$>$PVA$>$PMEAVH$>$Povacoat F$>$ PA-HCL$>$PEI$>$Poloxamer 188$>$PAA coumarin 6-SAs.

Most of the Poly/PTX-SA exhibited negative zeta potential (between −4.34 to −13.1 mV, Fig. 1 B) while PA-HCl (+9.54 mV) and PEI (+3.09 mV) exhibited positive zeta potential.

To further screen all these Poly/PTX-SAs for cancer therapeutics, a suitable self-assembly formulation must be hemocompatible. This property is highly recommended for any clinically applied or approved formulation. The safety profile of PTX-SAs on RBCs for hemocompatibility was examined at 10 μg/well of PTX or Poly/PTX-SAs. Results suggests that PVP, PVA, PA-HCl, and Poloxamer 188 based PTX-SAs exhibited negligible hemolysis (similar to negative control treatment, PBS) while other PTX-SAs demonstrated higher hemolysis (more than 20% hemolysis) like a free PTX drug (Fig. 2A). This hemocompatibility behavior with PVP and PVA is correlated with intact membrane morphology in RBCs just like a negative control (PBS) treated RBCs (Fig. 2B). All other Poly/PTX-SAs exhibited severe influence on shape and morphology of RBCs (Fig. 2B). PTX alone exhibited significant toxic behavior by disintegrating membrane structure of RBCs.

Irrespective of the type of drug formulation, they must interact and penetrate through the cell membrane of cancer cells, then be released into the cytosol at sufficient concentrations to induce therapeutic benefit. Therapeutic outcomes are improved if the intracellular uptake of nanoparticle is improved. Thus, higher internalization of formulation in the cells is the key factor to determine the efficiency of the nanoparticle formulation. The cellular uptake was conducted using dye-loaded polymer assemblies which can be assessed by green fluorescence in cells which directly reflects the internalization of the formulation. This study demonstrated an uptake of coumarin 6 pattern in MDA-MB-231 cells as PVP > PVA > PMEAVH > Povacoat F > PA-HCL > PEI > Poloxamer 188 > PAA PTX-SAs, whereas similar pattern was observed in MCF7 cells with the highest cellular uptake in PVP/PTX-SA (Fig. 3A). The mean fluorescence intensities of PVP/PTX-SAs and PVA/PTX-SA were ~16 and 14; ~10 and 9 times higher in MDA-MB-231 and MCF7, respectively (Fig. 3A). Fluorescence images of cells provide further evidence for similar uptake characteristics of polymer self-assemblies than that observed in flow cytometry. PVP and PVA self-assemblies were clearly detected in cancer cells all over the cellular organelles while other polymers show less fluorescence in these cells (Fig. 3B). However, the higher size range of PVA/PTX-SA of 358.86 nm, minimized the chances of using it as a potential nanoformulation. Thus we selected PVP/PTX-SAs for the rest of the study, as PVP is a better binder for transporting loaded therapeutics into cancer cells.

From the DLS, hemocompatibility, and cellular uptake studies, it can be reported that PVP/PTX self-assemblies have the optimal size and negative charge while maintaining hemocompatibility and improved cellular uptake in cancer cells that are may be helpful for
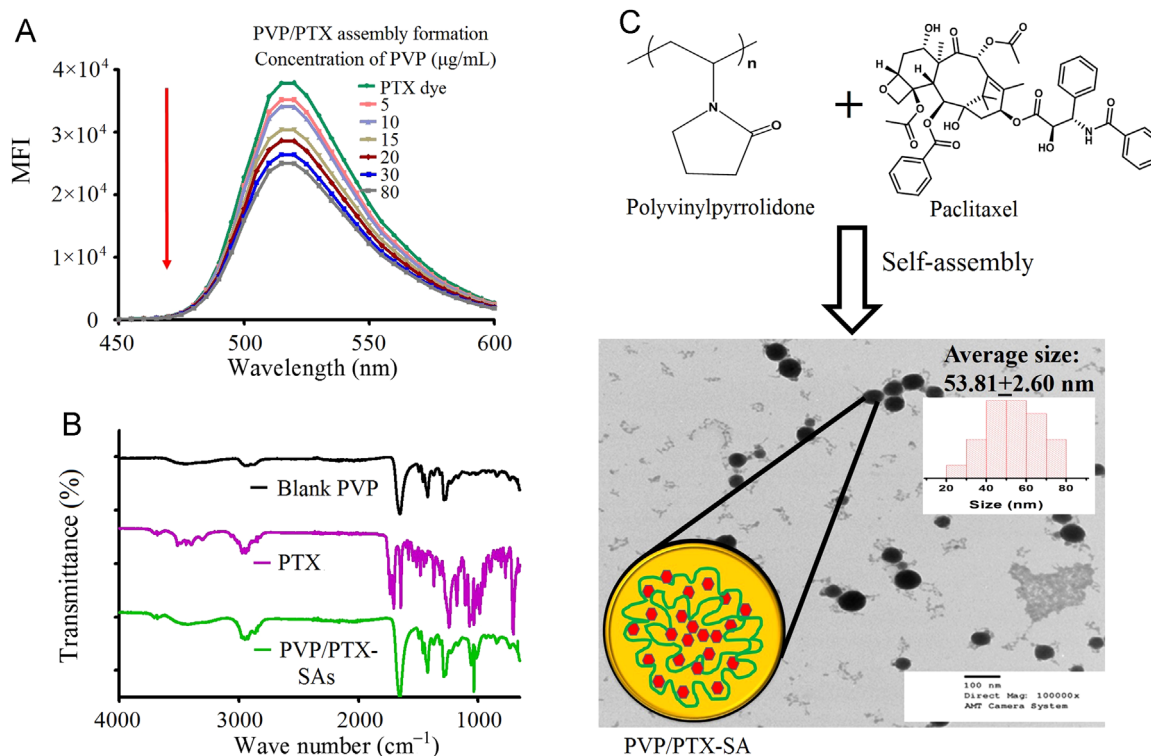

Figure 4 Self-assembly formation of PVP/PTX-SAs. A) Self-assembly formation was confirmed by binding potential (quenching) of PTX conjugated dye (PTX, Oregon Green 488 conjugate (Flutax-2, Molecular Probes Inc., Life Technology, OR, USA)) with PVP solution (5–80 μg/mL). Fluorescence was studied by exciting at 496 nm and emission between 450–600 nm. (B) FTIR spectra of PVP/PTX-SAs, PTX, and PVP. The presence of 1033 cm^{-1} (characteristic PTX peak) and 1270, 1284, 1420 and 1654 cm^{-1} characteristic PVP peak) confirms the presence of both PVP and PTX in the self-assembly formation of PVP/PTX-SAs. (C) Schematic and hypothetical structural presentation of PVP/PTX-SAs. Color, dimensions, assembly are not comparable to synthesized formulation. Morphology of PVP/PTX-SAs imaged by using AMT camera at a direct magnification of 100,000× under the TEM on a 150 mesh standard TEM grid, stained by 2% *w/v* uranyl acetate solution. The average particle size viewed under TEM 53.81 ± 2.6 nm. (For interpretation of the references to color in this figure legend, the reader is referred to the web version of this article.)

cancer therapeutic purposes. Thus, all our further studies described in this manuscript are focused on PVP/PTX-SAs.

3.2. Characterization of PVP/PTX self-assembly formation

In order to confirm that PVP and PTX form self-assembly nanoparticles, we utilized PTX-conjugated dye (PTX, Oregon Green 488 conjugate) for fluorescence quenching assay. In the first method, to confirm efficient binding of PTX with the PVP, a quenching study was performed against PTX-conjugated dye (PTX, Oregon Green 488 conjugate) in 1× PBS solution (Fig. 4A). Fluorescence quenching reveals possible interaction of polymer with PTX dye. This is instantaneous process directly couples/self-assembles PTX to polymer. Such instantaneous particle formation and integrity was confirmed by hydrodynamic diameter measurements using DLS. The fluorescence intensity of PTX dye was diminished with increase of PVP solution. This directly correlates to the binding potential of PVP with PTX which indicates successful formation of self-assemblies.

The inclusion of PVP and PTX in PVP/PTX-SAs can be confirmed using FTIR analysis. The FTIR spectra of the PVP, PTX, and PVP/PTX-SAs (Fig. 4B) demonstrate that PTX has distinct visible peaks at 1734 cm^{-1}, 1704 cm^{-1} and 1645 cm^{-1} (due to C = O stretching of amide and ester functionality) which were not visible in PVP/PTX-SA thus suggesting a possible interaction of PVP with PTX through these functional groups. Further, in the PVP/PTX-SAs spectrum, the intensity of the broad band around 3259 cm^{-1} was reduced suggesting another possible interaction

motif with the alcoholic O–H functionality too. If we look into the fingerprint region of the FTIR spectrum for the PVP/PTX-SAs formulation, the sharp peak at 1033 cm^{-1} confirms the presence of PTX in the formulation. Lastly, the peaks at 1270, 1284, 1420 and 1654 cm^{-1} of both PVP/PTX-SA and PTX substantiates the coexistence of both PVP and PTX in the given formulation. The FTIR study was performed to confirm the existence of polymer and PTX in its formulation but not to verify the course of self-assembly formation between polymer and PTX. Additional evidence is to examine its nanoparticle formation using TEM for the size and the morphology of self-assemblies (Fig. 4C). A clear contrast of self-assembled nanoparticles formation was observed with positively stained (2% w/v uranyl acetate solution) PVP/PTX-SAs. From this study, it is evident that the average size of the dry and stained PVP/PTX-SAs found to be $53.81 \pm 2.6 \text{ nm}$. DLS data provides particles in suspension or wet form which always exhibit higher particle size over TEM measurements. This nanoparticle observation substantiates and affirms the hydrodynamic size of the nanoparticles measured by DLS.

3.3. In vitro anticancer potential of PVP/PTX-SAs

The therapeutic efficacy of PVP/PTX-SAs was evaluated in breast cancer cell lines by MTS viability and colony formation assay[32]. Both PTX and PVP/PTX-SAs showed a dose-dependent antiproliferation effect (1.25–20 nmol/L) in MCF7 and MDA-MB-231 (Fig. 5A). The control polymer did not show any effect on cell growth. The in vitro 50% cell growth inhibitory concentration (IC_{50})
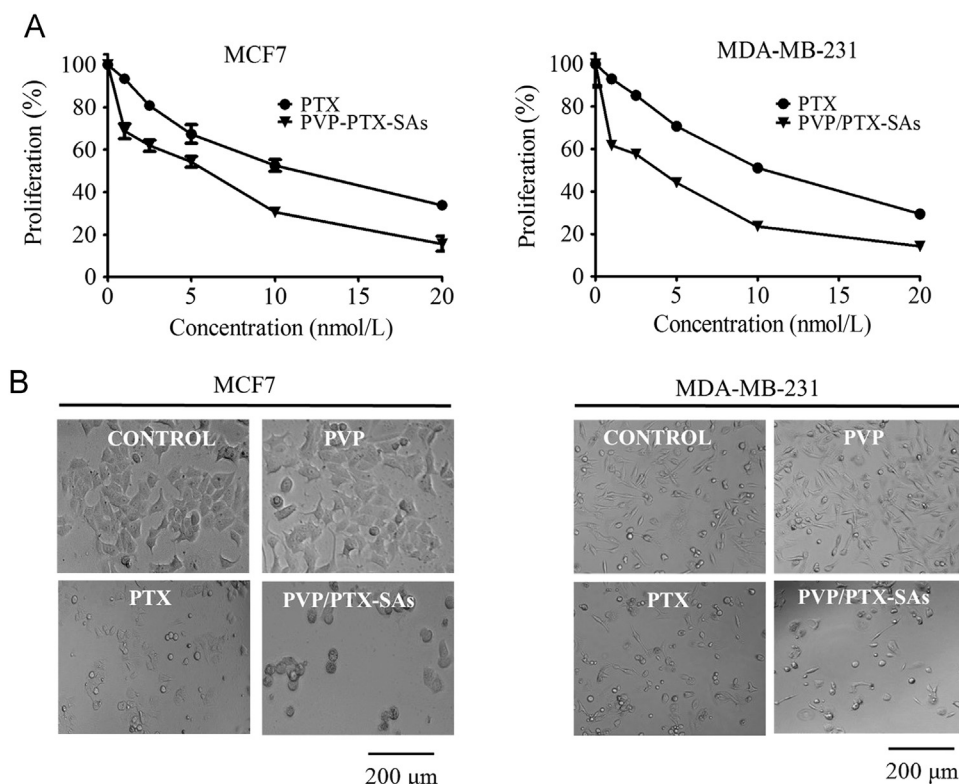

Figure 5 PVP/PTX-SAs significantly inhibit proliferation of breast cancer cells. (A) Breast cancer cells (MCF7 and MDA-MB-231, 5000 cells/well) were plated in 96-well plate and were treated with PTX or PVP/PTX-SA at a range of concentration 1–20 nmol/L for 48 h. Cell viability was assessed by MTS assay by measuring absorbance at 490 nm using microplate reader. Relative cell viability was measured (using GraphPad Prism 5 Software) with control (untreated) breast cancer cells, considering as 100%. Data represented as mean $\pm$ standard error of the mean ($n = 3$), $^*P < 0.05$. (B) Representative phase contrast microscopic images were captured by EVOS® FL Imaging System to evaluate the effect of PVP/PTX-SAs on the cell morphology. PTX or PVP/PTX-SA concentration was equivalent to 5 PTX nmol/L. Bar equals to 200 μm.
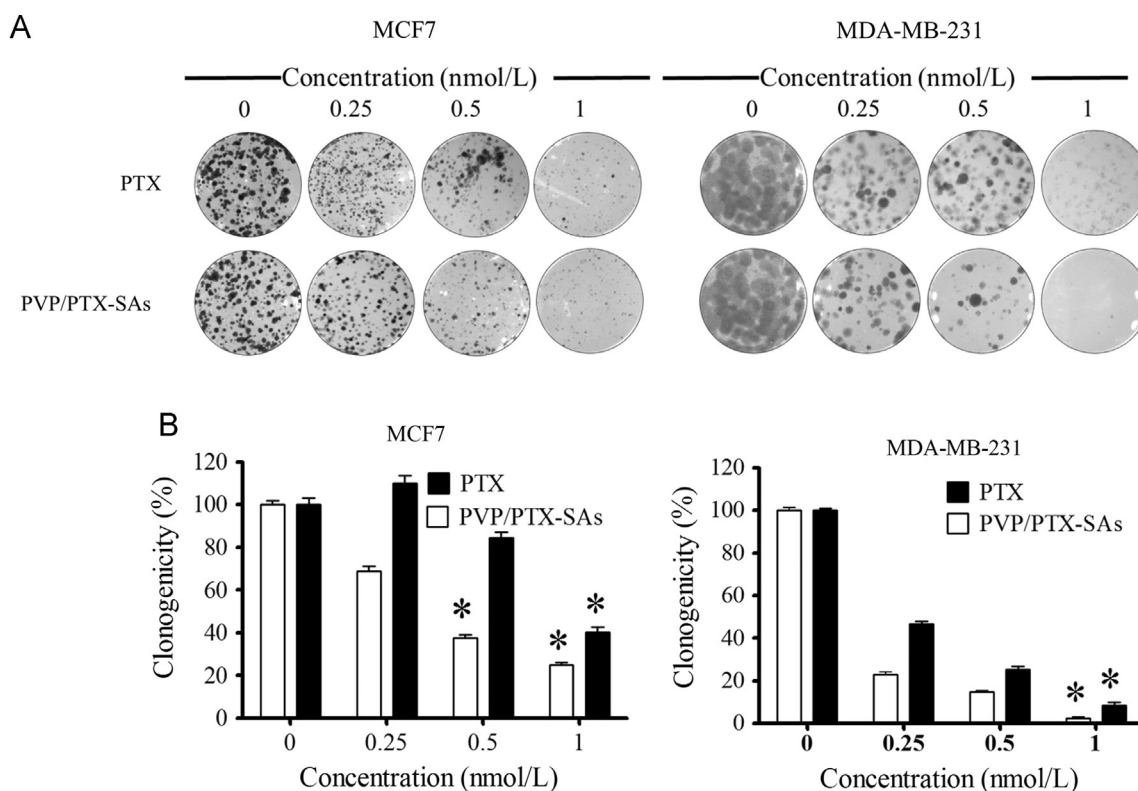
Figure 6 PVP/PTX-SAs repress the clonogenic potential of breast cancer cells. (A) Breast cancer cells (MCF7 and MDA-MB-231, 250 cells/well in a 12-well plate) were treated with 0.25, 0.5, and 1 nmol/L PVP/PTX-SAs and PTX along with their respective controls. On day 14, cells were rinsed with PBS and stained with hematoxylin to visualize colonies for counting. Photographs of clonogenic pattern were captured in Multimage™ light cabinet. (B) Bar graphs represent number of colonies formed in each treatment group. Data represented as mean $\pm$ standard error of the mean ($n = 3$), $^*P < 0.05$.

is the quantitative measure of the toxicity induced by treatment group on the cells. IC_{50} values for PTX is 13.12 nmol/L and 12.40 whereas IC_{50} for PVP/PTX-SAs is 4.68 and 7.26 nmol/L, for MCF7 and MDA-MB-231, respectively. Similarly, images of treated cells indicate that the inherent anticancer activity of PTX is preserved in PVP/PTX-SAs (Fig. 5B). In fact, PVP/PTX-SA formulation is more potent in suppressing cell growth compared to PTX. A similar superior active performance of PVP/PTX-SAs was achieved in the colony forming assay, which is another complementary assay to evaluate anticancer efficacy (Fig. 6). In this study, PVP/PTX-SAs have shown a significant decrease in colonies and colony density over PTX for both MCF7 and MDA-MB-231 (Fig. 6A and B). Such high anti-proliferative and colonogenic potency of PVP/PTX-SAs at a low effective dose compared to paclitaxel demonstrates that a lesser concentration of PTX is needed in self-assembly formulations for effective therapeutic outcomes.

3.4. Molecular activity of PVP/PTX-SAs

At the cellular level, PTX binds to the β-tubulin subunits in microtubules and induces polymerization of tubulin which disrupts microtubule dynamics, may causing mitotic arrest and thus cell death[37]. To obtain further insight in this aspect of PVP/PTX-SAs, we performed β-tubulin stabilization using a specific antibody in immunostaining and imaging by confocal microscopy. A higher

microtubule polymer mass was observed on treatment with PVP/PTX-SAs, in contrast with PTX (5 and 10 nmol/L) or respective control groups (DMSO or PVP). Higher microtubule bundles in cells, suggested by the green fluorescence observed for microtubule staining (Fig. 7A), is due to enhanced antitumor activity of PVP/PTX-SAs compared to PTX. This behavior was more prominent even at 10 nmol/L (Data not shown) concentration with PVP/PTX-SAs indicating the use of PVP/PTX-SAs may reduce concentrations required to induce anticancer effect.

We performed immunoblot analysis to further understand the superior anticancer function of PVP/PTX-SAs in breast cancer cells. Expression of various proteins such as BCL-XL, BID, BAX, cleaved PARP, cleaved caspase 7, and MDR1 upon treatment with PTX and PVP/PTX-SAs was assessed (Fig. 7B). The expression of key pro-survival protein (BCL-XL) was effectively down-regulated by PTX and PVP/PTX-SAs treatment. In addition, expression of pro-apoptosis proteins (BAX and BID), cleaved PARP, and cleaved caspase 7, increased following PTX and PVP/PTX-SAs treatment. These events are more prominent in PVP/PTX-SAs strongly suggests PVP/PTX-SAs induce apoptosis more pronouncedly in comparison to the native drug PTX[38]. Further, the effect of treatment on MDR1 protein expression was also observed. Altogether, we can conclude that PVP/PTX-SAs were able to stabilize tubulin polymerization and cause intrinsic differences in molecular effects, which could effectively induce apoptosis.
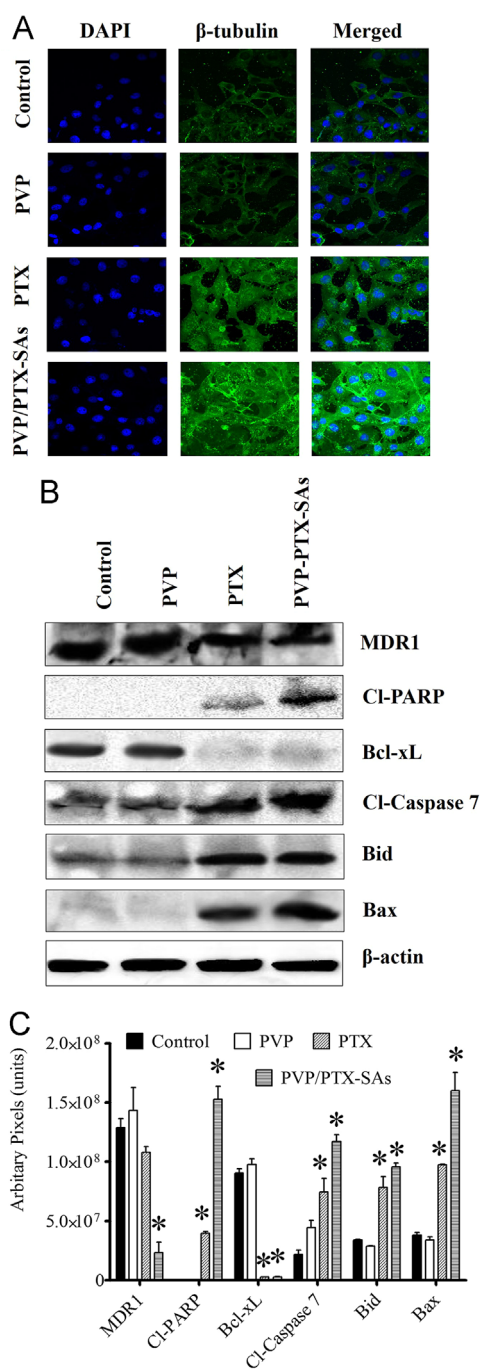
Figure 7 Preferential cell death induced by PVP/PTX-SAs in MDA-MB-231 cells. (A) Tubulin stabilization images of polyvinylpyrroli-done paclitaxel self-assembly. Cells have been treated with equivalent concentrations of 5 nmol/L PTX or PVP/PTX-SA for 8 h. Imaged by Carl Zeiss LSM 710. Original magnification 400×. This data suggests PVP/PTX-SA treatment leads to PTX-induced microtubule stabilization. (B) MDA-MB-231 cells were treated with 10 nmol/L PVP/PTX-SAs or PTX or respective controls for 48 h. Cell lysates were analyzed to detect levels of Bax, Bid, cleaved caspase 7, cleaved PARP, Bcl-xL, and MDR1, with β-actin as a control. (C) Densitometry analysis of Bid, Bax, cleaved caspase 7, cleaved PARP, Bcl-xL, and MDR1 in MDA-MB-231 cells after 48 h treatment with 10 nmol/L PVP/PTX-SAs or PTX and their respective controls. The results were consistent in two independent sets of experiments.

4. Discussion

The main problem of paclitaxel-based chemotherapy is severe systemic toxicity due to nonspecific accumulation of anticancer agent. In other words, administration of paclitaxel with lipophilic solvents or surfactant(s) may result in insufficient drug levels at the tumor site or quick clearance due to the aggregation of paclitaxel nanoformulation. Although literature and clinical evidence suggest some formulations have exhibited superior therapeutic outcome, a simple preparative approach like self-assembly formulations of paclitaxel is preferred[39,40]. Therefore, the main focus of this study is to develop paclitaxel/polymer based nanoformulations by self-assembly technique to enhance the efficacy of paclitaxel in breast cancer treatment. Polymeric nanoparticles are better alternatives for drug delivery with improved therapeutic benefits. In this same regard, we prepared nanoparticle colloidal system with paclitaxel entrapped in the matrix. The unique structure of the polymeric matrix provides advantages of delivery and intracellular penetration. Thus achieving sustained drug release, preventing frequent administration and overall broad spectrum of therapeutic benefits are expected[41]. The unique preparative approach of self-assembly technique enables formulation scientists to reduce usage of external excipients and in the process reduces the chances of toxicity from the nanocarrier itself. It is reported that the superiority of self-assembled nanoparticles in the field of drug delivery is favored[39,40]. The hydrophilic aqueous polymeric solution serves as a bed for the hydrophobic drug through van der Waals forces/interaction or hydrogen bonding at the core of the particle. Hydrophobic interaction between the hydrophobic polyvinyl group of PVP and paclitaxel is responsible in the formation of the nanoformulation. Due to steric stabilization, these nanodrug formulations have a longer retention in the blood stream whereas their nanosized structures facilitate the nanoformulation to escape through the leaky vasculature and release of drug at the tumor sites owing to their enhanced permeability and retention effect[42]. Self-assembled drug nanoparticles have gained significant interest in the therapeutic field due to biocompatibility[43], biodegradability, and low immunogenic properties[44,45]. Therefore, in this study, we examined the ability of eight commonly used pharmaceutical polymers to generate Poly/PTX-SAs. Among these eight polymers, PVP polymer was not only capable of producing the smallest size (140.53 nm) with a negative zeta potential (–6.21 mV, Fig. 1). This formulation was also exhibited lower toxicity with RBCs (Fig. 2) than PTX alone. Additionally, these PVP-coumarin 6-SAs exhibited superior interaction with breast cancer cells compared to other Poly/coumarin 6-SAs (Fig. 3). The size and zeta potential properties of the PVP/PTX-SAs formulation resembles clinically-used PTX nanoparticle formulations such as Abraxane® and Genexol® PM. A negative zeta potential, favorable for the stability of the nanoparticles, prevent them from binding to the plasma proteins and prolong their circulation[46]. Due to these physicochemical characteristics delivery can be avoided. As it is the inherent nature of these nanoparticles, they may tend to reach at the tumor site via enhanced permeation and retention effect[47]. However, there was no direct evidence provided through this article. The self-assembly formation of PVP and PTX was further confirmed by TEM (particle assembly leads to 53.81 nm) and a continuous dose-dependent binding profile with paclitaxel in fluorescence quenching experiments (Fig. 4). From the spectral analysis, it is confirmed that the presence of chemical functional/repeating units of PVP and PTX in PVP/PTX-SAs that are found
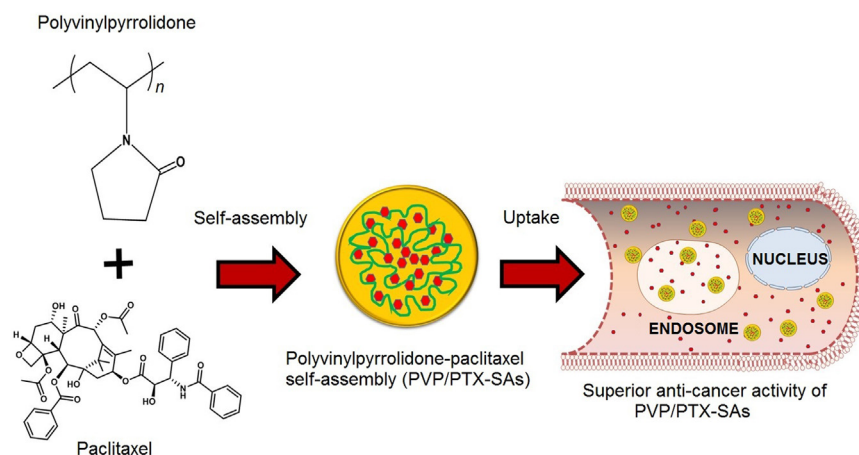
Scheme 1 Schematic and hypothetical structural representation of PVP/PTX-SAs. Color, dimensions and assembly are not comparable to synthesized formulation. (For interpretation of the references to color in this figure legend, the reader is referred to the web version of this article.)

in the particles, suggesting that the integrity of the polymer(s) and PTX is maintained in the formulation.

Polyvinylpyrrolidone is widely used as inactive pharmaceutical excipient for binder/disperser, film former, flavoring liquid, and adhesive applications for multiple uses such as tablets, capsules, ophthalmic solution, and transdermal patches. Earlier in 1950s, PVP was used as a plasma volume expander. More importantly, PVP is considered as generally safe chemical for many uses by the U.S. Food and Drug Administration. Thus, it may hold promise in delivering PTX too. PVP was earlier implemented as a binder/stabilizer for PTX in a reverse microemulsion[48], solvent evaporation[49] and nanoprecipitation methods for PTX/PVP-PCL nanoparticles (110 nm)[50,51]. These studies support our current findings that PVP is a better choice for holding PTX in self-assembly grooves. PVP has been used as a solid dispersion for PTX and docetaxel[52,53]. In addition, Sharma et al.[48] also developed polyvinylpyrrolidone nanoparticle-encapsulated taxol. Our approach is a direct self-assembly or solid dispersion method while above formulation is based on reverse microemulsion method. Based on our study, we believe that self-assembly of PVP and PTX may happen due co-precipitation.

In order to further utilize PVP as a self-assembly binder or delivery carrier for PTX, it is crucial for the nanoparticle to interact more closely with cancer cells and release effectively into cytosol for maximizing the pharmacological effects of PTX. Through this study, we proved that the PVP/PTX-SAs induce a greater amount of formulation in cancer cells as observed with fluorescence microscopy and flow cytometry (Fig. 3). In addition, PVP/PTX-SAs exhibit superior anticancer activity in proliferation and clonogenic assays against breast cancer cells, compared to PTX alone (Figs. 5 and 6).

PTX is a classical and unquestioned microtubule inhibitor which exhibits clinical success. PTX promotes tubulin polymerization and stabilization of microtubules resulting in G2-M phase arrest and thus mitotic cell death occurs[54]. Development of improved tubulin-binding drugs or improving PTX tubulin-binding and improving the stability of microtubule efficiency with formulations of any type are considered to be attractive in cancer therapeutics. In this investigation, we observed that our lead PVP/PTX-SAs are acting significantly on cell tubulin dynamics and tubulin polymerization, thus contributing to mitotic block in breast cancer cells (Fig. 7A)[55]. This determines the impact of PVP's role in this formulation as a drug carrier. In cancer therapeutics,

apoptosis induced by the Bcl-2 family is an important parameter as it allows prediction of the mitochondrial pathway[56]. In this regard, our study results showed distinct effects of PVP/PTX-SAs on apoptotic signaling with reduced expression of Bcl-xL, profound expression of pro-apoptotic proteins (Bax and Bid), and the expression profile of cleaved PARP, and cleaved caspase 7, in comparison to control and native drug treatments. This demonstrates that enhanced apoptotic cell death occurs with PVP/PTX-SAs treatment than with conventional exposure[57]. These results further affirm enhanced toxicity effects of prepared samples and are well consistent with the results of proliferation and clonogenic assays.

Altogether, PVP/PTX-SAs demonstrated that these nanoparticles are taken up by breast cancer cells, and induce superior anticancer activity in breast cancer cells (Scheme 1). Further, PVP is known to provide extensive stability to the therapeutic molecules and reduction of renal clearance[58]. These data support the feasibility of developing PVP/PTX-SAs as nanoparticle-based therapeutics for improving the therapeutic benefits of PTX. The shortcome of this study is that there is no direct evidence that our nanoformulation is directly targeting tumor cells. However, in our future work, we plan design this PVP/PTX-SAs as targeted drug delivery technology employing our targeted delivery protocols[27,30,33]. Developing such targeted nanoformulation is aimed for intravenous administration. That way we can achieve higher therapeutic benefits of such self-assembly nanoparticle formulation through targeted approachability.

5. Conclusions

Introducing clinically relevant PTX (hydrophobic anticancer drug) into self-assembled nanoparticles was successfully achieved. Based on particle size, cellular uptake, and hemolysis assays, PVP/PTX-SAs were found to be better formulations over seven other Poly/PTX-SAs. We observed superior anticancer effects of PVP/PTX-SAs through inhibition of proliferation and colony formation, which were further confirmed by tubulin stabilization and immunoblot analysis. These findings highlight the advantages of implementation of PVP/PTX-SAs in comparison to other conventional PTX formulations. However, further pre-clinical evidence is needed to confirm the advantages for cancer patients of such self-assembly systems and to gain mechanistic insights.

Acknowledgements

Appendix A.   Supplementary material

Supplementary data associated with this article can be found in the online version at http://dx.doi.org/10.1016/j.apsb.2017.10.004.

References

1. Siegel RL, Miller KD, Jemal A. Cancer statistics, 2017. *CA Cancer J Clin* 2017;**67**:7–30.
2. Sofias AM, Dunne M, Storm G, Allen C. The battle of "nano" paclitaxel. *Adv Drug Deliv Rev* 2017http://dx.doi.org/10.1016/j.addr.2017.02.003.
3. Donehower RC. The clinical development of paclitaxel: a successful collaboration of academia, industry and the National Cancer Institute. *Stem Cells* 1996;**14**:25–8.
4. Montero AJ, Adams B, Diaz-Montero CM, Glück S. Nab-paclitaxel in the treatment of metastatic breast cancer: a comprehensive review. *Expert Rev Clin Pharmacol* 2011;**4**:329–34.
5. Brouwer E, Verweij J, De Bruijn P, Loos WJ, Pillay M, Buijs D, et al. Measurement of fraction unbound paclitaxel in human plasma. *Drug Metab Dispos* 2000;**28**:1141–5.
6. Gelderblom H, Verweij J, Nooter K, Sparreboom A. Cremophor EL: the drawbacks and advantages of vehicle selection for drug formulation. *Eur J Cancer* 2001;**37**:1590–8.
7. Di Costanzo F, Gasperoni S, Rotella V, Di Costanzo F. Targeted delivery of albumin bound paclitaxel in the treatment of advanced breast cancer. *Onco Targets Ther* 2009;**2**:179–88.
8. ten Tije AJ, Verweij J, Loos WJ, Sparreboom A. Pharmacological effects of formulation vehicles: implications for cancer chemotherapy. *Clin Pharmacokinet* 2003;**42**:665–85.
9. van Zuylen L, Verweij J, Sparreboom A. Role of formulation vehicles in taxane pharmacology. *Invest New Drugs* 2001;**19**:125–41.
10. Mustacchi G, De Laurentiis M. The role of taxanes in triple-negative breast cancer: literature review. *Drug Des Devel Ther* 2015;**9**:4303–18.
11. Hamaguchi T, Matsumura Y, Suzuki M, Shimizu K, Goda R, Nakamura I, et al. NK105, a paclitaxel-incorporating micellar nanoparticle formulation, can extend *in vivo* antitumour activity and reduce the neurotoxicity of paclitaxel. *Br J Cancer* 2005;**92**:1240–6.
12. Oasmia pharmaceutical announces positive over all survival results from phase III study of Paclical/Apealea for treatment of ovarian cancer[April 27, 2016]. Available from ⟨http://oasmia.com/en/press-release/oasmia-pharmaceutical-announces-positive-overall-survival-results-phase-iii-study-paclicalapealea-treatment-ovarian-cancer/⟩.
13. Koudelka Š, Turánek J. Liposomal paclitaxel formulations. *J Control Release* 2012;**163**:322–34.
14. Jain MM, Gupte SU, Patil SG, Pathak AB, Deshmukh CD, Bhatt N, et al. Paclitaxel injection concentrate for nanodispersion *versus* nab-paclitaxel in women with metastatic breast cancer: a multicenter, randomized, comparative phase II/III study. *Breast Cancer Res Treat* 2016;**156**:125–34.
15. Havel H, Finch G, Strode P, Wolfgang M, Zale S, Bobe I, et al. Nanomedicines: from bench to bedside and beyond. *AAPS J* 2016;**18**:1373–8.
16. Zhang JA, Anyarambhatla G, Ma L, Ugwu S, Xuan T, Sardone T, et al. Development and characterization of a novel Cremophor® EL free liposome-based paclitaxel (LEP-ETU) formulation. *Eur J Pharm Biopharm* 2005;**59**:177–87.
17. Hasenstein JR, Shin H-C, Kasmerchak K, Buehler D, Kwon GS, Kozak KR. Antitumor activity of Triolimus: a novel multidrug-loaded micelle containing paclitaxel, rapamycin, and 17-AAG. *Mol Cancer Ther* 2012;**11**:2233–42.
18. Rösler A, Vandermeulen GW, Klok H-A. Advanced drug delivery devices *via* self-assembly of amphiphilic block copolymers. *Adv Drug Deliv Rev* 2001;**53**:95–108.
19. Xu L, Ma W, Wang L, Xu C, Kuang H, Kotov NA. Nanoparticle assemblies: dimensional transformation of nanomaterials and scalability. *Chem Soc Rev* 2013;**42**:3114–26.
20. Mai Y, Eisenberg A. Self-assembly of block copolymers. *Chem Soc Rev* 2012;**41**:5969–85.
21. Kabanov AV, Batrakova EV, Alakhov VY. Pluronic® block copolymers for overcoming drug resistance in cancer. *Adv Drug Deliv Rev* 2002;**54**:759–79.
22. Suk JS, Suh J, Choy K, Lai SK, Fu J, Hanes J. Gene delivery to differentiated neurotypic cells with RGD and HIV Tat peptide functionalized polymeric nanoparticles. *Biomaterials* 2006;**27**:5143–50.
23. Cassagneau T, Fendler JH, Mallouk TE. Optical and electrical characterizations of ultrathin films self-assembled from 11-aminoundecanoic acid capped TiO_2 nanoparticles and polyallylamine hydrochloride. *Langmuir* 2000;**16**:241–6.
24. Kumar RV, Koltypin Y, Cohen YS, Cohen Y, Aurbach D, Palchik O, et al. Preparation of amorphous magnetite nanoparticles embedded in polyvinyl alcohol using ultrasound radiation. *J Mater Chem* 2000;**10**:1125–9.
25. Grzelczak M, Vermant J, Furst EM, Liz-Marzán LM. Directed self-assembly of nanoparticles. *ACS Nano* 2010;**4**:3591–605.
26. Lin Y, Böker A, He J, Sill K, Xiang H, Abetz C, et al. Self-directed self-assembly of nanoparticle/copolymer mixtures. *Nature* 2005;**434**: 55–9.
27. Nagesh PKB, Johnson NR, Boya VKN, Chowdhury P, Othman SF, Khalilzad-Sharghi V, et al. PSMA targeted docetaxel-loaded superparamagnetic iron oxide nanoparticles for prostate cancer. *Colloids Surf B Biointerfaces* 2016;**144**:8–20.
28. Boya VN, Lovett R, Setua S, Gandhi V, Nagesh PK, Khan S, et al. Probing mucin interaction behavior of magnetic nanoparticles. *J Colloid Interface Sci* 2017;**488**:258–68.
29. Dobrovolskaia MA, Clogston JD, Neun BW, Hall JB, Patri AK, McNeil SE. Method for analysis of nanoparticle hemolytic properties *in vitro*. *Nano Lett* 2008;**8**:2180–7.
30. Yallapu MM, Foy SP, Jain TK, Labhasetwar V. PEG-functionalized magnetic nanoparticles for drug delivery and magnetic resonance imaging applications. *Pharm Res* 2010;**27**:2283–95.
31. Karthik S, Kumar BNP, Gangopadhyay M, Mandal M, Singh NDP. A targeted, image-guided and dually locked photoresponsive drug delivery system. *J Mater Chem B* 2015;**3**:728–32.
32. Yallapu MM, Jaggi M, Chauhan SC. β-Cyclodextrin-curcumin self-assembly enhances curcumin delivery in prostate cancer cells. *Colloids Surf B Biointerfaces* 2010;**79**:113–25.
33. Yallapu MM, Khan S, Maher DM, Ebeling MC, Sundram V, Chauhan N, et al. Anti-cancer activity of curcumin loaded nanoparticles in prostate cancer. *Biomaterials* 2014;**35**:8635–48.
34. Rajput S, Puvvada N, Kumar BNP, Sarkar S, Konar S, Bharti R, et al. Overcoming Akt induced therapeutic resistance in breast cancer through siRNA and thymoquinone encapsulated multilamellar gold niosomes. *Mol Pharm* 2015;**12**:4214–25.
35. Yallapu MM, Jaggi M, Chauhan SC. Poly(β-cyclodextrin)/curcumin self-assembly: a novel approach to improve curcumin delivery and its therapeutic efficacy in prostate cancer cells. *Macromol Biosci* 2010;**10**:1141–51.

36. Puvvada N, Rajput S, Kumar BN, Mandal M, Pathak A. Exploring the fluorescence switching phenomenon of curcumin encapsulated niosomes: *in vitro* real time monitoring of curcumin release to cancer cells. *RSC Adv* 2013;**3**:2553–7.

37. Jordan MA, Wilson L. Microtubules and actin filaments: dynamic targets for cancer chemotherapy. *Curr Opin Cell Biol* 1998;**10**:123–30.

38. Kwon G, Suwa S, Yokoyama M, Okano T, Sakurai Y, Kataoka K. Enhanced tumor accumulation and prolonged circulation times of micelle-forming poly (ethylene oxide-aspartate) block copolymer-adriamycin conjugates. *J Control Release* 1994;**29**:17–23.

39. Klok HA, Lecommandoux S. Supramolecular materials *via* block copolymer self-assembly. *Adv Mater* 2001;**13**:1217–29.

40. Qin SY, Zhang AQ, Cheng SX, Rong L, Zhang XZ. Drug self-delivery systems for cancer therapy. *Biomaterials* 2017;**112**:234–47.

41. Chowdhury P, Nagesh PK, Kumar S, Jaggi M, Chauhan SC, Yallapu MM. Pluronic nanotechnology for overcoming drug resistance. In: Yan B, Zhou H, Gardea-Torresdey J, editors. *Bioactivity of Engineered Nanoparticles*. Singapore: Springer; 2017. p. 207–37.

42. Cho H-J, Yoon I-S, Yoon HY, Koo H, Jin Y-J, Ko S-H, et al. Polyethylene glycol-conjugated hyaluronic acid-ceramide self-assembled nanoparticles for targeted delivery of doxorubicin. *Biomaterials* 2012;**33**:1190–200.

43. Yadav AK, Agarwal A, Rai G, Mishra P, Jain S, Mishra AK, et al. Development and characterization of hyaluronic acid decorated PLGA nanoparticles for delivery of 5-fluorouracil. *Drug Deliv* 2010;**17**:561–72.

44. Cui W, Li J, Decher G. Self-assembled smart nanocarriers for targeted drug delivery. *Adv Mater* 2016;**28**:1302–11.

45. Shi J, Xiao Z, Kamaly N, Farokhzad OC. Self-assembled targeted nanoparticles: evolution of technologies and bench to bedside translation. *Acc Chem Res* 2011;**44**:1123–34.

46. Huang J, Zhang H, Yu Y, Chen Y, Wang D, Zhang G, et al. Biodegradable self-assembled nanoparticles of poly (D,L-lactide-*co*-glycolide)/hyaluronic acid block copolymers for target delivery of docetaxel to breast cancer. *Biomaterials* 2014;**35**:550–66.

47. Farokhzad OC, Langer R. Impact of nanotechnology on drug delivery. *ACS Nano* 2009;**3**:16–20.

48. Sharma D, Chelvi TP, Kaur J, Chakravorty K, De TK, Maitra A, et al. Novel Taxol formulation: polyvinylpyrrolidone nanoparticle-encapsulated Taxol for drug delivery in cancer therapy. *Oncol Res* 1996;**8**:281–6.

49. Gaucher G, Poreba M, Ravenelle F, Leroux J-C. Poly(*N*-vinyl-pyrrolidone)-block-poly(D,L-lactide) as polymeric emulsifier for the preparation of biodegradable nanoparticles. *J Pharm Sci* 2007;**96**:1763–75.

50. Xu H, Hou Z, Zhang H, Kong H, Li X, Wang H, et al. An efficient Trojan delivery of tetrandrine by poly(*N*-vinylpyrrolidone)-block-poly(ε-caprolactone) (PVP-*b*-PCL) nanoparticles shows enhanced apoptotic induction of lung cancer cells and inhibition of its migration and invasion. *Int J Nanomed* 2014;**9**:231–42.

51. Zhu Z, Li Y, Li X, Li R, Jia Z, Liu B, et al. Paclitaxel-loaded poly(*N*-vinylpyrrolidone)-*b*-poly(ε-caprolactone) nanoparticles: preparation and antitumor activity *in vivo*. *J Control Release* 2010;**142**:438–46.

52. Liu X, Sun J, Chen X, Wang S, Scott H, Zhang X, et al. Pharmacokinetics, tissue distribution and anti-tumour efficacy of paclitaxel delivered by polyvinylpyrrolidone solid dispersion. *J Pharm Pharmacol* 2012;**64**:775–82.

53. Sawicki E, Beijnen JH, Schellens JH, Nuijen B. Pharmaceutical development of an oral tablet formulation containing a spray dried amorphous solid dispersion of docetaxel or paclitaxel. *Int J Pharm* 2016;**511**:765–73.

54. Rowinsky EK, Cazenave LA, Donehower RC. Taxol: a novel investigational antimicrotubule agent. *J Nat Cancer Inst* 1990;**82**:1247–59.

55. Jordan MA, Wilson L. Microtubules as a target for anticancer drugs. *Nat Rev Cancer* 2004;**4**:253–65.

56. Antonsson B, Martinou J-C. The Bcl-2 protein family. *Exp Cell Res* 2000;**256**:50–7.

57. Guo D-D, Moon H-S, Arote R, Seo J-H, Quan J-S, Choi Y-J, et al. Enhanced anticancer effect of conjugated linoleic acid by conjugation with Pluronic F127 on MCF-7 breast cancer cells. *Cancer Lett* 2007;**254**:244–54.

58. Kamada H, Tsutsumi Y, Yamamoto Y, Kihira T, Kaneda Y, Mu Y, et al. Antitumor activity of tumor necrosis factor-*α* conjugated with polyvinylpyrrolidone on solid tumors in mice. *Cancer Res* 2000;**60**:6416–20.